A STRATIFIED-THEORETICAL CALCULATION MODEL
OF CONCRETE UNDER EXTERNAL SULFATE ATTACK

YUE LI[1], ZHONGZHENG GUAN[1], ZIGENG WANG[1] *, PENG WANG[1], GUOSHENG ZHANG[1], QINGJUN DING[2]

[1] *Key Laboratory of Urban Security and Disaster Engineering of Ministry of Education, Beijing Key Laboratory of Earthquake Engineering and Structural Retrofit, Beijing University of Technology, Beijing, 100124, China.*
[2]*State Key Laboratory of Advanced Technology for Materials Synthesis and Processing, Wuhan University of Technology, Wuhan, 430070, China.*

This paper presents an integrated investigation of deterioration process of corroded concrete by experiments and theoretical model. First of all, the porosities of concrete samples with different corrosion periods were measured by the mercury intrusion porosimetry (MIP). Then the distribution of sulfate ions in the concrete was measured by the spectrophotometric method. Afterwards, the compressive strength were measured. The results indicated that the porosity and the compressive strength of concrete in water firstly increased and then progressively stabilized at a constant value due to the hydration of cement. However, those values of concrete soaked in 5wt.% Na_2SO_4 solution increased and then decreased, resulted from the combination of cement hydration and the corrosion of sulfate ions. Moreover, a Stratified-Theoretical calculation model was established with the input parameters of corrosion depth of sulfate ion, length of concrete specimen, strength of concrete immersed in water and in sulfate solution. At last, the corrosion resistance coefficient of corrosion layer was firstly put forward to evaluate the deterioration process of concrete with high effectiveness.

1. Introduction

Concrete is the most commonly material used in construction field. As known, sulfate as a corrosive media, was one of the most destructive objectives for concrete [1]. Therefore, the studies on deterioration mechanism and properties variation of concrete caused by sulfates has been conducted for decades.

Owing to chemical shrinkage, dry shrinkage, autogenous shrinkage and loading, the micro-cracks developed in concrete inevitably [2-5]. When concrete contacted with external sulfate solution, the sulfate ionic concentration gradient between the external solution and the internal solution of concrete formed, resulting in the progressive diffusion of sulfate ions from high concentration zones to low concentration zones through the cracks and the pore structures [6,7]. Studies [8-11] pointed that the external sulfate ions reacted with the cement hydration products to generate ettringite and gypsum. As ettringite and gypsum grew, the swelling stress gradually exceeded the ultimate tensile strength of the concrete, causing further cracking. Moreover, the new generating micro cracks accelerated the transport of sulfate ions and

the deterioration process of concrete [12].

Clifton [13] established a chemical-mechanical analysis model to study the relationship between the volume change of expansive products and the strain in the cement-based material under sulfate attack. Additionally, many scholars [14-21] built transport–chemical-mechanical models in the basis of the volume change caused by the resultants (ettringite and gypsum) and the transport characteristics of sulfate ions to quantitatively predict the deterioration process and the mechanical properties of concrete attacked by sulfate. However, the existing models cannot accurately reveal the damage evolution of concrete due to a lot of unresolved issues, such as subsequent corrosion of concrete, decalcification of C-S-H , leaching of portlandite [22,23] and crystal growth of mirabilite [24].

In this study, the mercury intrusion porosimetry (MIP), the distribution of sulfate ions and the compressive strength were measured. In order to accurately describe the damage evolution of concrete, the corroded cubic concrete samples were divided into corrosion layer and non-corrosion layer and a Stratified-Theoretical calculation model was established. At last, the corrosion resistance

---
* Autor corespondent/*Corresponding author*,
E-mail: zigengw@bjut.edu.cn

Table 1

Mineral composition of cement.

Composition	C_3S	C_2S	C_3A	C_4AF
Content(%)	63.94	16.79	7.41	11.86

Table 2

Mix proportion of concrete samples.

W/C	Water(kg/m^3)	Cement(kg/m^3)	Sand(kg/m^3)	Gravel(kg/m^3)
0.53	200	375	750	1125

coefficient were calculated to evaluate the deterioration process of the concrete.

2. Materials and sample preparation
2.1. Materials

P•I 52.5 Portland cement was used in this study with the mineral compositions shown in Table 1. Natural river sand with fineness modulus of 2.7 and mud content of less than 1 wt.% was utilized. The size distribution of the gravel was 5~20 mm and the mixing water was tap water. The mix design of the concrete is shown in Table 2.

2.2. Sample preparation

The original concrete sample was cubic with a dimension of 100 mm×100 mm×100 mm. All the samples were stored at 20±2°C for 24h before demolding, then cured for 7 d with standard curing condition (20±2°C, relative humidity of 95%). In order to obtain the one-dimensional distribution of sulfate ions in corroded concrete samples, two opposite faces of each sample were exposed to air and the other four surfaces were sealed with epoxy resin before immersed in solutions. The samples were divided into two groups, including immersed in Na_2SO_4 solutions with the concentration of 0 wt.% (water) and 5 wt.% at 20±2°C for different periods. The Na_2SO_4 solution was replaced every 7 d to ensure a constant concentration.

In this study, three different experiments were conducted, including MIP, distribution of sulfate ions and compressive strength. For MIP test, the selection and preparation of the concrete samples is shown in Fig. 1. Firstly, the concrete cubic sample was perpendicularly cut with the corroded surface as shown in Fig. 1 (a). Then a

small cubic samples with 10 mm×10 mm×10 mm was cut off from the cubic sample as shown in Fig. 1 (b). Fig. 1 (c) exhibits the sample for MIP test. In order to obtain the distribution of sulfate ions, the powders of each sample were obtained by a concrete bench drill with the sampling depth of 0 mm, 1.5 mm, 3.5 mm, 7.5 mm, 12.5 mm, 17.5 mm, 22.5 mm and corrosion periods of 0 d, 30 d, 120 d. For the uniaxial compression test, 3 cubic concrete samples were selected for each group with the corrosion period of 0 d, 10 d, 20 d, 30 d, 40 d, 60 d, 90 d, 120 d, 150 d and 180 d, meaning 60 samples in total.

3. Experimental analysis
3.1. Porosity

An Auto Pore IV9500 mercury intrusion porosimeter (MIP) produced by MICROMERITICS Co., USA was used to measure the porosity of the concrete samples. Fig. 2 shows that the porosities of the concrete samples over corrosion periods. The porosity of concrete samples soaked in water decreases promptly at the early stage (before 60 d) because of the further hydration of cement. After 60 d, the rate of corrosion significantly decreases and the porosity of concrete stabilizes at approximate 13.65% because the hydration of cement gradually completed over time. However, the porosity of concrete samples immersed in 5 wt.% Na_2SO_4 solution drops faster than that soaked in water at the early stage, caused by the combination of the hydration of cement and the generation of expansive products. Then the porosity reaches the lowest value of approximate 7.86% at 60 d, decreasing by about 45% of the porosity (14.27%) of concrete samples soaked in
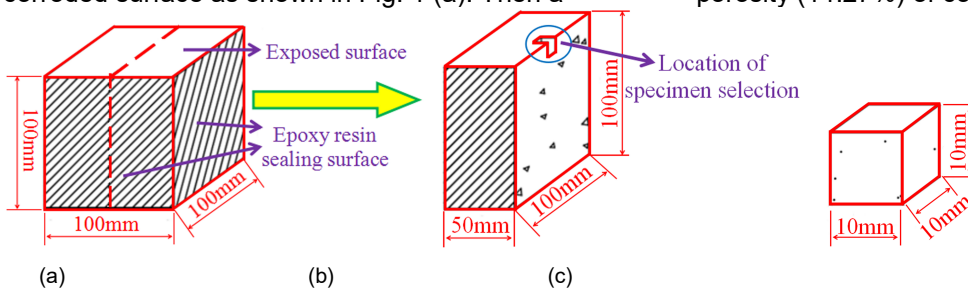

Fig. 1 - Samples selection and preparation: (a) Concrete sample; (b) Cutting perpendicularly to the exposed surface; (c) Samples for SEM and MIP.

water with the same period. With increase of the corrosion time, the porosity gradually exceeds the value of the water group. The porosity of the concrete sample in 5 wt.% Na_2SO_4 solution is 14.42% at 120 d, which is greater than that in water at 120 d with the value of 13.67%. The difference between the porosity of concrete sample in 5 wt.% Na_2SO_4 solution and that in water is 4.87% at 180 d.
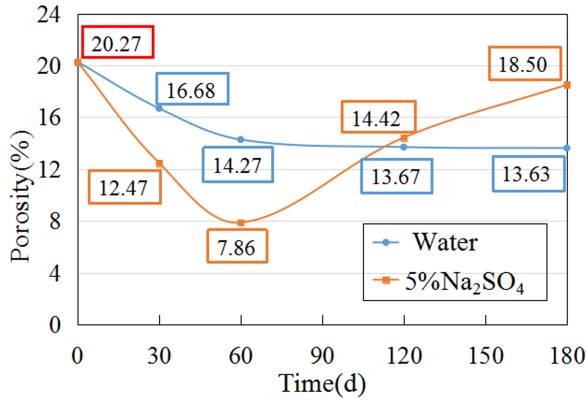

Fig. 2 - Variation in the concrete's porosity over time.

3.2. Distribution of sulfate ions

The spectrophotometric method was adopted to measure the mass fraction of sulfate ions in concrete samples in this section. Fig. 3 shows the concentration variation of sulfate ions in the concrete samples with different corrosion periods. Firstly, the concentration of sulfate ions in concrete sample with corrosion period of 0 d is approximate 0.3% due to original sulfate ions existing in the cement. After the corrosion of 30 d, the concentration of sulfate ions in the sample surface is 1.5% which is much higher than that in

the interior of concrete sample. In addition, with the increase of depth to the sample surface, the concentration of sulfate ions decreases, reaching to a stable value of 0.3%. The corrosion depths of sulfate ions in concrete samples with corrosion periods of 30 d and 120 d are 9.49 mm and 16.44 mm, respectively. It can be found that the concentration of sulfate ions in the concrete sample at the same depth increases with the time of corroded in 5 wt.% Na_2SO_4 solution.
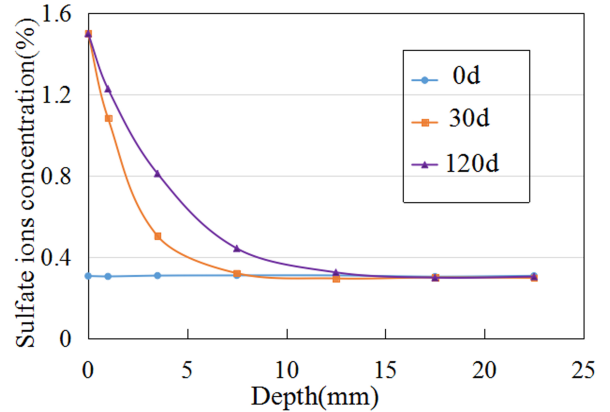

Fig. 3 - Distribution of sulfate ions in concrete.

3.3. Compressive strength

The compressive strength of the cubic concrete samples was tested by a microcomputer - controlled electro - hydraulic servo pressure testing machine (YAW6303) with a constant loading of 0.5 MPa. Table 3 shows the compressive strengths of concrete samples with different corrosion periods. It is seen that f_w and f_c are the average compressive strengths of concrete samples in water and 5 wt.% Na_2SO_4 solution, respectively. S_{fw} and S_{fc} are the standard

Table 3

The compressive strength of concrete samples

f (MPa)	f_{w1}	f_{w2}	f_{w3}	f_w	S_{fw}	f_{c1}	f_{c2}	f_{c3}	f_c	S_{fc}
0d	33.45	36.08	34.27	34.60	1.35	33.45	36.08	34.27	34.60	1.35
10d	38.68	37.92	42.98	39.86	2.73	43.13	41.06	39.83	41.34	1.67
20d	42.39	45.28	46.52	44.73	2.12	45.63	48.21	47.82	47.22	1.39
30d	47.65	46.89	48.08	47.54	0.60	50.35	52.25	51.57	51.39	0.96
40d	48.06	48.86	49.33	48.75	0.64	54.62	57.86	53.39	55.29	2.31
60d	49.15	47.96	49.56	48.89	0.83	57.28	59.26	58.06	58.20	1.00
90d	47.69	48.58	50.52	48.93	1.45	54.92	52.36	55.17	54.15	1.56
120d	48.27	49.56	48.66	48.83	0.66	50.05	52.26	49.88	50.73	1.33
150d	49.69	50.58	47.75	49.34	1.45	46.18	48.82	50.35	48.45	2.11
180d	50.69	48.39	48.88	49.32	1.21	46.56	44.89	47.33	46.26	1.25

deviations of the compressive strengths of the concrete samples in water and 5 wt.% Na_2SO_4 solution, respectively. The standard deviations within 2.5 are much smaller than the average values, indicating that the data are reliable. The compressive strength of concrete samples soaked in water undergoes a process of increasing first, then gradually stabilizing at a constant of 48.8 MPa. However, the compressive strength of concrete samples in 5 wt.% Na_2SO_4 solution rapidly increases at the early stage, reaching peak of 58.2 MPa at 60 d. Compared to the group of concrete samples in water, the compressive strength soaked in 5 wt.% Na_2SO_4 solution increases by 21.7% at 60 d. After corroded of 60 d, the compressive strength of the concrete sample decreases and the value is lower than that soaked in water after 150 d. With the increase of soaking time, the downward trend develops more apparently. It can be deduced that the compressive strength of concrete samples are consistent with the changes of the porosity [25].

4. Establishment of the Stratified-Theoretical calculation model

In this section, the mechanism basis is the Fick's second law of diffusion, the modified sulfate ion diffusion coefficient and the corrosion depth of sulfate ions obtained from the first two factors. Then based on the corrosion depth of sulfate ions, the concrete attacked by sulfate is divided into non-corrosion layer and corroded layer. Subsequently, a Stratified-Theoretical calculation model was established with the input parameters of corrosion depth of sulfate ion, the length of concrete specimen, the strength of concrete immersed in water and in sulfate solution. The output results of the model were the compressive strength of the corroded layer and the corrosion resistance coefficient of concrete attacked by sulfate.

4.1. Calculation of sulfate ion diffusion coefficient and corrosion depth

The Fick's second law of diffusion was used to describe the transport behavior of sulfate ions in Na_2SO_4 solution. The sulfate concentration can be expressed as

$$C(x,t) = C_0 + (C_s - C_0)\left[1 - erf\left(\frac{x}{2\sqrt{Dt}}\right)\right] \quad (1)$$

where $C(x,t)$ represents the sulfate concentration of the sample with depth of x below the surface at time t, %. t is the diffusion time, d. C_0 is the initial concentration of sulfate ions in concrete, %, C_0 =0.3. C_s denotes the surface concentration of sulfate ions, %, C_s =1.5. D is the sulfate ion diffusion coefficient, mm²/d. In this study, D was calculated based on the sulfate ions concentrations of the seven points at 30 d in Fig. 3. For the point (1.5,1.054), the variable $D(1.5,30)$ was calculated as 0.123 mm²/d at 30 d by Eq.(1). Then the other

six values of D were calculated, averaged as 0.122 mm²/d at 30 d. In the same way, D was 0.099 mm²/d at 120 d. In addition, when $C(x,30)=0$, the corrosion depth of sulfate ions was 9.21 mm at 30 d by Eq. (1). The corrosion depth of sulfate ions can be calculated by Eq. (2) [26]

$$h = \sqrt{\frac{2Dct}{a}} \quad (2)$$

where h is the corrosion depth of sulfate ions, mm. c is the mass concentration of sulfate ions in the solution, %. a is the capacity of concrete to absorb sulfate ions. Given $c=0.05$, $t=30$d, $D=0.122$mm²/d and $h=9.21$mm, a was calculated as 4.315×10^{-3}.

Owing to the hydration of cements and the complicated physical and chemical behaviors of sulfate ions in concrete, the changes of the pore structure and porosity led to the variation of concrete density. Thus, the diffusion coefficient of sulfate ion changed over time. So the time variation coefficient m was introduced to optimize D, as shown in Eq. (3)

$$D_t = D_0\left(\frac{t_0}{t}\right)^m \quad (3)$$

where D_t is the diffusion coefficient of sulfate ions at time t, mm²/d. D_0 is the diffusion coefficient of sulfate ions at time t_0, mm²/d. m is the time variation coefficient. Given $t_0=30$ d, $D_0=0.122$ mm²/d, t=120 d, $D_{120}=0.099$ mm²/d, m was calculated as 0.13. Then Eq. (3) can be expressed as

$$D_t = 0.122\left(\frac{30}{t}\right)^{0.13} \quad (4)$$

The change in the sulfate ion corrosion depth h can be obtained from Eqs. (2) and (4). The theoretical values and experiment values of the sulfate ion corrosion depth are shown in Fig. 4. The sulfate ion corrosion depth of the theoretical values are 9.21 mm and 16.63 mm at 30 d and 120 d, which are close to the experiment values 9.49 mm and 16.44 mm at 30 d and 120 d, respectively. Therefore, the theoretical values can be used as the corrosion depth for the following section.
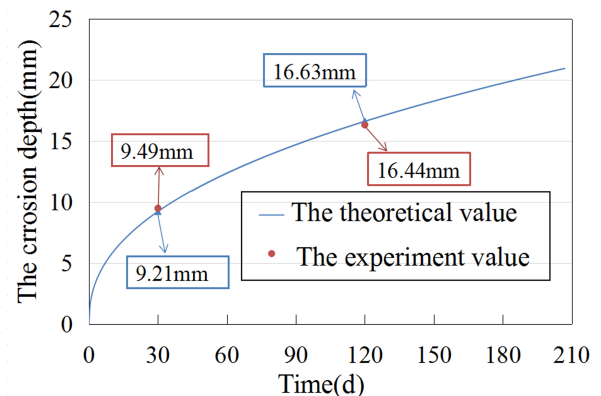

Fig. 4 - Variation in the erosion depth of SO_4^{2-} over time.

4.2. Establishment of the Stratified-Theoretical calculation model based on the corrosion depth

The sulfate ions reacted with hydration products of cement to create expansive productions in the concrete. With the amount of expansive productions increasing, the same region of the concrete experienced the process from densifying to cracking. Due to the sulfate ion diffusion, the corrosion of concrete occurred from the exterior to the interior and the corrosion layer of concrete progressively thickened. In order to establish the Stratified-Theoretical calculation model and obtain the corrosion resistance coefficient of the corrosion zone of the concrete samples, the following assumptions were drawn:

1) The initial micro-pores and micro-cracks were uniformly distributed in the concrete matrix.

2) The cubic concrete sample was defined as non-corrosion layer I_0 and corroded layer I_f (dense zone I_{f1} and cracking zone I_{f2}).

3) The expansion and the damage from the reaction between sulfate ions and hydration products of cement in the concrete were uniform in the same layer.

In the early stage of cement hydration, sulfate ions diffused into the concrete surface, reacting with Ca^{2+} and $[Al(OH)]^{2+}$ in pore solution to form ettringite and gypsum as the expansive products filling the pore structure of the concrete surface zone and enhancing the degree of compactness. This stage was called strengthening stage and the corresponding zone experiencing this process was called dense zone, I_{f1} (Fig. 5 (a)). Subsequently, the corrosion depth of sulfate ions gradually increased and the dense zone of concrete migrated into the interior of concrete. Meanwhile, the ettringite crystallites gradually grew to trigger the swelling stress and micro-cracks in the external region around the dense zone, turning the external area of the dense zone into cracking zone, shown in Fig. 5 (b). Fig. 5 (c) displays the sulfate-attacked concrete sample with corrosion layer and non-corrosion layer. This stage was called deterioration stage. In the strengthening stage, the corrosion zone of the concrete was the dense zone. In the deteriorating stage, the corrosion zone of the concrete was the dense zone plus cracking zone.

The corrosion depth of sulfate ions can be used as an effective parameter to evaluate the mechanical properties of concrete corrosion zone [1]. The chemical reaction rate of sulfate ions was much faster than the diffusion rate [1, 26]. Then the thickness of corrosion layer of concrete d_f can be obtained from the corrosion depth by Eq.(5).

$$d_f = h \qquad (5)$$

where d_f is the thickness of concrete corrosion layer and h is the corrosion depth of sulfate ions, mm.

According to Fig. 5 (c), the compressive strength of concrete under external sulfate attack can be expressed as:

$$f_c = \frac{f_0 A_0 + f_f A_f}{A} \qquad (6)$$

where f_c, f_0, and f_f are the compressive strength of the total zone, non-corrosion layer and corrosion layer of concrete subjected to sulfate attack, MPa, respectively. f_w is the compressive strength of concrete in water, so $f_0 = f_w$. A, A_0, and A_f are the area of the entire zone, non-corrosion layer and corrosion layer of concrete, mm^2, respectively. In this study, $A = L^2$, $A_0 = (L - 2d_f)^2$, $A_f = A - A_0 = 4h(h - d_f)$. Moreover, the model can be used as the cylinder specimen by changing the length of concrete cubic specimen L to the diameter of concrete cylinder specimen R. The chemical reaction rate of sulfate ions was much faster than the diffusion rate [1, 21]. The compressive strength of the concrete corrosion layer obtained by Eq. (6) is:

$$f_f = \frac{f_c A - f_w A_0}{A_f} \qquad (7)$$

The compressive strength variation of the corrosion layer was the result of the hydration of cement paste and the corrosion of sulfate ions. Then the change of compressive strength in corrosion layer caused by sulfate ions is:

$$f_S = f_f - f_w \qquad (8)$$

where f_s is the change of compressive strength in the corrosion layer, MPa. To describe the change in compressive strength of the concrete corrosion layer over time, the corrosion resistance coefficient of concrete is defined as
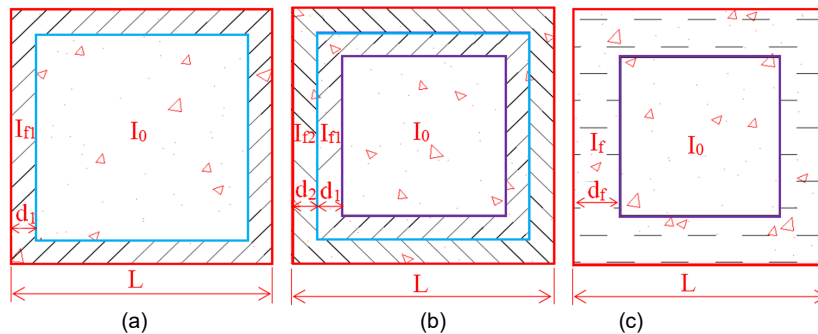

Fig. 5 - The corrosion process of concrete: (a) The strengthening stage; (b) The deterioration stage; (c) The schematic diagram.

Table 4

The compressive strength f_f and the corrosion resistance coefficient k_f of the concrete corrosion layer.

t(d)	h(mm)	f (MPa)			k_f (%)
		f_w	f_c	f_f	
0	0.00	34.6	34.6	--	--
10	5.90	39.86	41.34	46.52	--
20	7.76	44.73	47.22	53.43	20
30	9.21	47.54	51.39	59.13	29
40	10.42	48.75	55.29	66.35	60
60	12.39	48.89	58.20	70.45	20
90	14.71	48.93	54.15	59.33	-37
120	16.63	48.83	50.73	52.26	-23
150	18.28	49.34	48.45	47.85	-16
180	19.75	49.32	46.26	44.49	-11

$$k_f = \frac{f_{S(n+1)} - f_{S(n)}}{T_{n+1} - T_n} \times 100\% \quad (9)$$

where k_f represents the corrosion resistance coefficient of concrete. $f_{S(n+1)}$ and $f_{S(n)}$ represent the change of compressive strength in the corrosion layer at time $T_{(n+1)}$ and $T_{(n)}$, MPa, respectively.

5. Analysis of corrosion mechanism based on the Stratified-Theoretical calculation model

Based on the Stratified-Theoretical calculation model, the corrosion depth of sulfate ion in Fig. 4 and the average values of the compressive strength in Table 3, the compressive strength f_f in the corrosion layer was calculated by Eqs. (7) and the corrosion resistance coefficient k_f was calculated by Eqs. (9). All the results are displayed in Table 4. It is observed that in 5 wt.% Na$_2$SO$_4$ solution, f_f firstly increases, reaching a maximum value of 70.45 MPa at 60 d, then dropping to the lowest value of 4.49 MPa at 180 d. k_f increases constantly in the first 40 d, indicating that compressive strength of the corrosion layer increases over time with an increasing growth rate at the strengthening stage. Then k_f with positive values noticeably reduces at 60 d, compared with the value at 40 d. It means that the compressive strength of the concrete corrosion layer still grows with a decreasing growth rate. After the corrosion period of 60 d, the concrete corrosion layer includes dense zone and cracking zone. After the corrosion of 90 d, the values of k_f are negative, indicating that the damage of concrete caused by the expansion cracking zone played a critical role and the concrete started to enter the deteriorating stage.

6. Conclusions

In this paper, MIP, distribution of sulfate ions and compressive strength of the concrete under sulfate attack were measured. Subsequently, a Stratified-Theoretical calculation model of concrete was established. Then the corrosion resistance coefficient as the output of the model was presented to evaluate the deterioration process of the concrete. The conclusions can be drawn as follows:

(1) The porosity variation of concrete soaked in water firstly increases and then progressively stabilizes at a constant value. However, the porosity variation of concrete soaked in 5wt.% Na$_2$SO$_4$ solution decreases after the initial increase.

(2) The variations of the compressive strength of concrete are essentially consistent with the change of the porosity variations of the corroded concrete.

(3) The corrosion resistance coefficient k_f can be used to precisely evaluate the deterioration process of concrete under Na$_2$SO$_4$ solution attack.

REFERENCES

1. Y. Zhou, et al., Strength Deterioration of Concrete in Sulfate Environment: An Experimental Study and Theoretical Modeling. Advances in Materials Science and Engineering, 2015. **2015**, 1.

2. Y. Li and J. Li, Capillary tension theory for prediction of early autogenous shrinkage of self-consolidating concrete. Construction and Building Materials, 2014. **53**, 511.

3. C.-H. Lu, H. Li, and R.-G. Liu, Chloride transport in cracked RC beams under dry–wet cycles. Magazine of Concrete Research, 2017. **69**(9), 453.

4. Z. Zhu, et al., Multi-scale modelling for diffusivity based on practical estimation of interfacial properties in cementitious materials. Powder Technology, 2017. **307**, 109.

5. Z. Wu, H.S. Wong, and N.R. Buenfeld, Influence of drying-induced microcracking and related size effects on mass transport properties of concrete. Cement and Concrete Research, 2015. **68**, 35.

6. S. Lorente, M.-P. Yssorche-Cubaynes, and J. Auger, Sulfate transfer through concrete: Migration and diffusion results. Cement and Concrete Composites, 2011. **33**(7), 735.

7. C. Lu, H. Li, and R. Liu, Chloride transport in cracked RC beams under dry–wet cycles. Magazine of Concrete Research, 2017. **69**(9), 453.

8. G. Rajasekaran, Sulphate attack and ettringite formation in the lime and cement stabilized marine clays. Ocean Engineering, 2005. **32**(8-9), 1133.

9. S.U. Al-Dulaijan, Sulfate resistance of plain and blended cements exposed to magnesium sulfate solutions. Construction and Building Materials, 2007. **21**(8), 1792.

10. J. Chen and M. Jiang, Long-term evolution of delayed ettringite and gypsum in Portland cement mortars under sulfate erosion. Construction and Building Materials, 2009. **23**(2), 812.

11. A. Bonakdar and B. Mobasher, Multi-parameter study of external sulfate attack in blended cement materials. Construction and Building Materials, 2010. **24**(1), 61.

12. M. Santhanam, M. Cohen, D, and J. Olek, Sulfate attack research—whither now? Cement and concrete research, 2001. **31**(6), 845.

13. J. Clifton, R and J. Pommersheim, M, Sulfate attack of cementitious materials volumetric relations and expansions. NIST IR, 1994. **5390**.

14. E. Rozière, et al., Durability of concrete exposed to leaching and external sulphate attacks. Cement and Concrete Research, 2009. **39**(12), 1188.

15. B. Bary, Simplified coupled chemo-mechanical modeling of cement pastes behavior subjected to combined leaching and external sulfate attack. International Journal for Numerical and Analytical Methods in Geomechanics, 2008. **32**(14), 1791.

16. M. Basista and W. Weglewski, Chemically Assisted Damage of Concrete: A Model of Expansion Under External Sulfate Attack. International Journal of Damage Mechanics, 2009. **18**(2), 155.

17. M. Basista and W. Weglewski, Micromechanical modelling of sulphate corrosion in concrete_ influence of ettringite forming reaction. heoretical and Applied Mechanics, 2008. **35**(1-3), 29.

18. A.E. Idiart, C.M. López, and I. Carol, Chemo-mechanical analysis of concrete cracking and degradation due to external sulfate attack: A meso-scale model. Cement and Concrete Composites, 2011. **33**(3), 411.

19. M. Shazali, M. Baluch, and A. Al-Gadhib, Predicting residual strength in unsaturated concrete exposed to sulfate attack. Journal of Materials in Civil Engineering, 2006. **18**(3), 343.

20. X.-B. Zuo, W. Sun, and C. Yu, Numerical investigation on expansive volume strain in concrete subjected to sulfate attack. Construction and Building Materials, 2012. **36**, 404.

21. B. Bary, et al., Coupled chemo-transport-mechanical modelling and numerical simulation of external sulfate attack in mortar. Cement and Concrete Composites, 2014. **49**, 70.

22. G. Geng, et al., Aluminum-induced dreierketten chain cross-links increase the mechanical properties of nanocrystalline calcium aluminosilicate hydrate. Sci Rep, 2017. **7**, 44032.

23. J.G. Wang, Sulfate attack on hardened cement paste. Cement and Concrete Research, 1994. **24**(4), 735.

24. N. Tsui, R. Flatt, J, and G. Scherer, W, Crystallization damage by sodium sulfate. Journal of cultural heritage, 2003. **4**(2), 109.

25. Z. Wu and H. Lian, High performance concrete. China railway Publishing House,Bei Jing, 2006.

26. S. Li, Y. Wang, and S. Wang, Research on the prediction model of concrete damage in the sulfate aggressive Environment. Journal of Wuhan University of Technology, 2010. **14**, 35.

****